

## **A Fluorescence Assay for Exosome Detection Based on Bivalent Cholesterol-Anchor Triggered Target Conversion and Enzyme-Free Signal Amplification**

Xiaokun Wang,<sup>†</sup> Hezhen Shang,<sup>‡</sup> Cuiping Ma,<sup>\*†</sup> Lingxin Chen<sup>\*§<sup>l</sup>#</sup>

<sup>†</sup> *Shandong Provincial Key Laboratory of Biochemical Engineering, College of Marine Science and Biological Engineering, Qingdao University of Science and Technology, Qingdao, 266042, PR. China.*

<sup>‡</sup> *Department of Hepatobiliary Surgery, Qingdao Chengyang District People's Hospital, Qingdao 266109, PR. China.*

<sup>§</sup> *CAS Key Laboratory of Coastal Environmental Processes and Ecological Remediation; Shandong Key Laboratory of Coastal Environmental Processes, Yantai Institute of Coastal Zone Research, Chinese Academy of Sciences, Yantai 264003, China.*

<sup>l</sup> *The Key Laboratory of Life-Organic Analysis, Key Laboratory of Pharmaceutical Intermediates and Analysis of Natural Medicine, College of Chemistry and Chemical Engineering, Qufu Normal University, Qufu 273165, China*

<sup>#</sup> *School of Pharmacy, Binzhou Medical University, Yantai 264003, China.*

Phone: +86-535-2109130 Fax: +86-535-2109130

\*Corresponding author: mcp169@163.com (C. Ma); E-mails: lxchen@yic.ac.cn (L. Chen)

## Table of Contents

### General experimental section

**Table S1.** Sequences of oligonucleotides used in this work.

**Figure S1.** Absorption intensities at 450 nm for bare (control) and anti-CD63 antibody-conjugated magnetic beads.

**Figure S2.** Optimization of experimental conditions. (a) Optimization of concentration ratios of H1 to H2. (b) Optimization of the incubation time for DNA circuitry.

**Figure S3.** (a) Absorption spectra response to different concentrations of exosomes. (b) Linear relationship between the absorption intensity ratio and logarithmic values of exosome concentrations.  $A$  and  $A_0$  refer to the absorption intensities with and without the addition of exosome, respectively.

**Figure S4.** Evaluation of assay specificity. (a) Normalized fluorescence spectra response to CD63 (2  $\mu\text{g/mL}$ ), TSG101 (2  $\mu\text{g/mL}$ ), CRP (2  $\mu\text{g/mL}$ ), BSA (2  $\mu\text{g/mL}$ ), and exosome ( $1.1 \times 10^6$  particles/ $\mu\text{L}$ ), respectively. (b) Corresponding fluorescence intensity to (a).

**Table S2.** Comparison among exosome detection methods.

**Table S3.** Recovery values of exosomes spiked into 20% diluted ED-FBS, 20% diluted UC-Serum, and 20% diluted UC-Urine by the proposed assay.

**Table S4.** Clinical information of healthy donors and cancer patients.

## General Experimental Section

**Instruments.** Native polyacrylamide gel electrophoresis (PAGE) was carried out using vertical electrophoresis systems (Beijing, China). Confocal microscopy fluorescence images were obtained by an Olympus FV1000. Transmission electron microscopy (TEM) image was acquired using a JEM-1230 instrument (JEOL, Tokyo, Japan). DS-11 Series UV-Vis Spectrophotometer (Wilmington, USA) and fluorescence spectrophotometer (F-7000, HITACHI) were used to obtain absorption and fluorescence spectral data, respectively. The annealing process was carried out by using PCR (Framingham, USA). The size and concentration of exosomes were obtained by using nanoparticle tracking analysis (NTA) at VivaCell Biosciences with ZetaView PMX 110 (Particle Metrix, Meerbusch, Germany) and corresponding software ZetaView 8.04.02.

**PAGE analysis of enzyme-free DNA circuits.** For the enzyme-free DNA circuits, the sequences were designed according to previous literature with a slight modification.<sup>1</sup> TNK buffer containing BC-anchor (5 nM), H1 (90 nM), H2 (135 nM), and RFQ (90 nM) was incubated for 2 h at room temperature. After different reaction products were prepared, 10  $\mu$ L of each sample was mixed with 2  $\mu$ L of 6 $\times$ loading buffer, then 10  $\mu$ L of the mixed solution was loaded into the lanes of a polyacrylamide gel. The gel was run at 180 V constant voltage for 2 min and then 135 V constant voltage for 70 min in 1 $\times$ TAE buffer at room temperature. After the gel was stained for 1 min in EtBr solution, it was photographed using the multifunctional imaging system.

**Exosome quantification by enzyme-linked immunosorbent assay (ELISA).** 30  $\mu$ L Anti-CD63 MBs were mixed with 20  $\mu$ L different concentrations of exosome and allowed to react under gentle shaking at room temperature. After 2 h, the mixture was washed three times with PBST and resuspended in PBS. 50  $\mu$ L anti-CD 63 rabbit antibody and anti-rabbit IgG-HRP were sequentially added to the immunocomplexes at an interval of 2 h. After incubation for another 1 h, the mixture was washed three times. Subsequently, 3,3',5,5'-tetramethylbenzidine (TMB) solution was added to induce the enzymatic reaction and TMB stop solution was added to terminate the reaction. Finally, the absorption spectra were measured by UV-Vis Spectrophotometer.

**Table S1.** Sequences of oligonucleotides used in this work.

Name	Sequence (5'-3')
<b>I</b>	<u>CGACATCTAACCTAGCTCACTGAC</u> ATAAGGCACGACGGCTTT-Cholesterol
<b>I<sub>c</sub></b>	Cholesterol-TTTGCCGTCGTGCCTTAT
<b>I<sub>AF</sub></b>	GTCAGTGAGCTAGGTTAGATGTCG-Alexa Fluor 488
<b>H1</b>	GTCAGTGAGCTAGGTTAGATGTCGCCATGTGTAGACGACATCTAACCTAGCCCTTGTCATAGAGCAC
<b>H2</b>	AGATGTCGTCTACACATGGCGACATCTAACCTAGCCCATGTGTAGA
<b>RF</b>	FAM-CGAGTGCTCTATGACAAGGGCTAGGTT
<b>RQ</b>	CCCTTGTCATAGAGCACTCG-Dabcyl

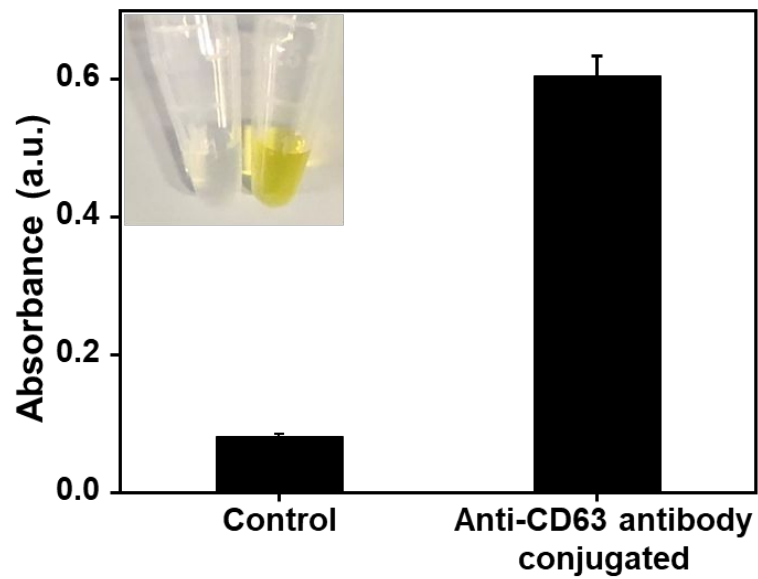


**Figure S1.** Absorption intensities at 450 nm for bare (control) and anti-CD63 antibody-conjugated magnetic beads.

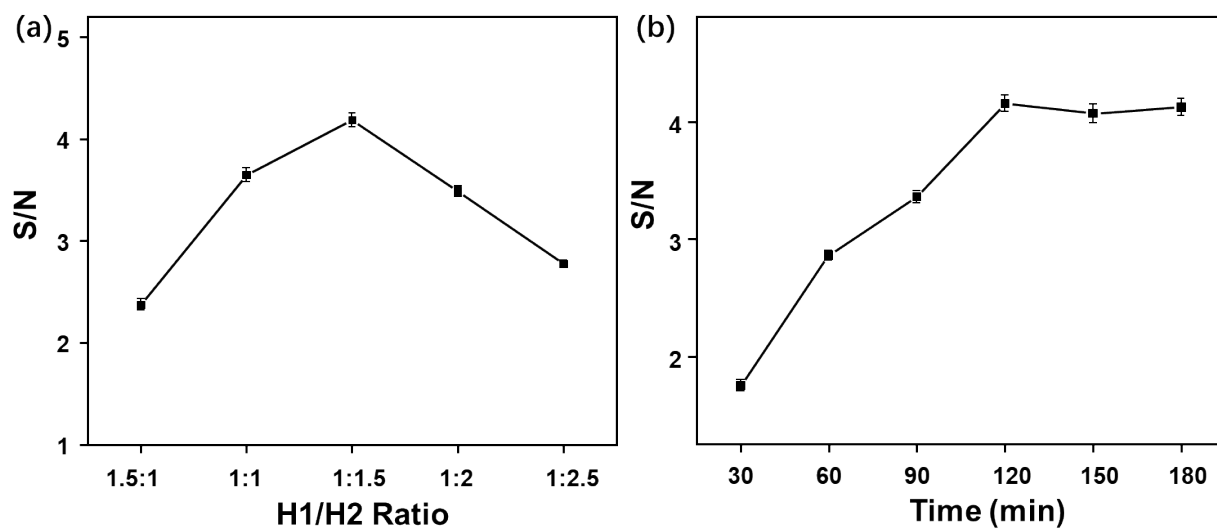


**Figure S2.** Optimization of experimental conditions. (a) Optimization of concentration ratios of H1 to H2. (b) Optimization of the incubation time for DNA circuitry.

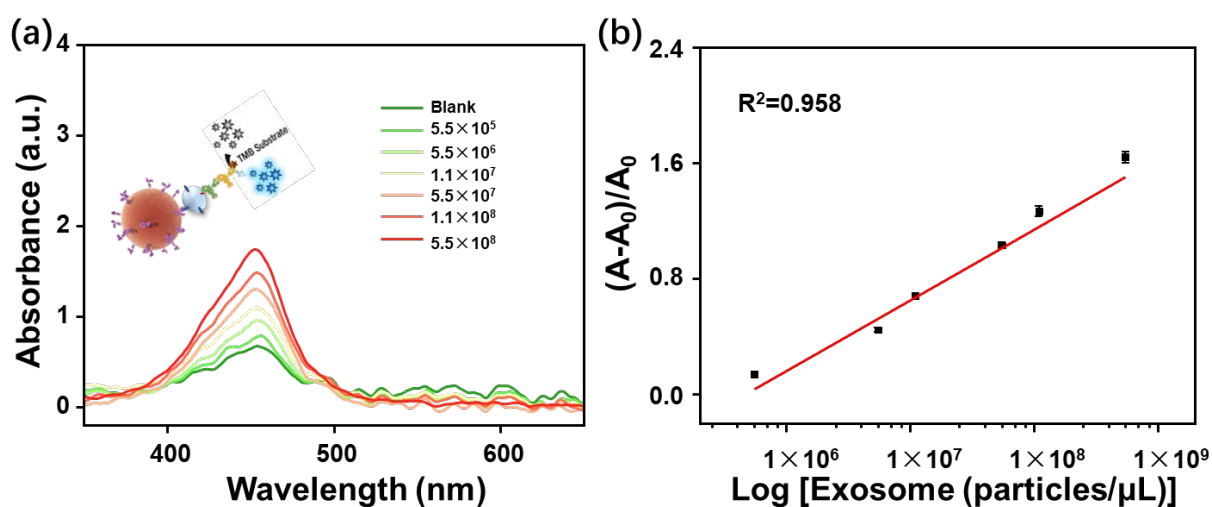


**Figure S3.** (a) Absorption spectra response to different concentrations of exosomes. (b) Linear relationship between the absorption intensity ratio and logarithmic values of exosome concentrations. A and  $A_0$  refer to the absorption intensities with and without the addition of exosome, respectively.

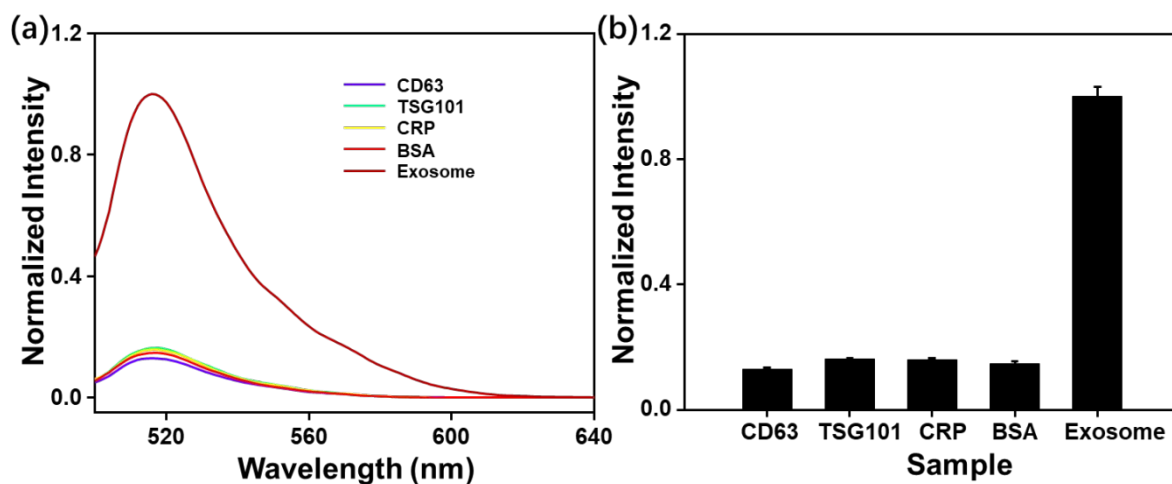


**Figure S4.** Evaluation of assay specificity. (a) Normalized fluorescence spectra response to CD63 (2  $\mu\text{g/mL}$ ), TSG101 (2  $\mu\text{g/mL}$ ), CRP (2  $\mu\text{g/mL}$ ), BSA (2  $\mu\text{g/mL}$ ), and exosome ( $1.1 \times 10^6$  particles/ $\mu\text{L}$ ), respectively. (b) Corresponding fluorescence intensity to (a).

**Table S2.** Comparison among exosome detection methods.

Detection Method	Identification Target	Linear Range (particles/ $\mu$ L)	Limit of Detection (particles/ $\mu$ L)	Real Sample	Reference
Colorimetry assay	CD63	$1.8 \times 10^6$ - $2.2 \times 10^7$	$5.2 \times 10^3$	Serum	2
Colorimetry assay	CD63 and CD9	$2.2 \times 10^5$ - $2.4 \times 10^7$	—	Serum	3
Paper-based aptasensor with LRET	CD63	$1.0 \times 10^4$ - $1.0 \times 10^8$	$1.1 \times 10^3$	—	4
SPRi-based biosensor	CD63	$3.1 \times 10^4$ - $1.0 \times 10^6$	$2.37 \times 10^4$	Serum	5
Lateral flow aptasensor	CD63	$1.0 \times 10^4$ - $1.0 \times 10^8$	$1.4 \times 10^4$	Serum	6
Fluorescent nanosensor	GPC-1	$7.8 \times 10^4$ - $3.9 \times 10^9$	$6.56 \times 10^4$	Serum	7
Fluorescent aptasensor	CD63 and bilipid layer	$7.5 \times 10^4$ - $1.5 \times 10^7$	$4.8 \times 10^4$	Serum	8
Fluorescent aptasensor	CD63	$1.0 \times 10^5$ - $1.0 \times 10^9$	$1.0 \times 10^5$	Serum	9
Electrochemical aptasensor	CD63	$1.12 \times 10^2$ - $1.12 \times 10^8$	96	Serum	10
Electrochemical enzymatic amplification	PSMA	$1.0 \times 10^3$ - $1.2 \times 10^5$ (particles)	70	FBS	11
Fluorescence biosensor with enzyme-free amplification	CD63 and bilipid layer	$5.5 \times 10^3$ - $1.1 \times 10^7$	$1.29 \times 10^3$	FBS/serum/urine	This Work

**Table S3.** Recovery values of exosomes spiked into 20% diluted ED-FBS, 20% diluted UC-Serum, and 20% diluted UC-Urine by the proposed assay.

Samples	Added (Particles/ $\mu\text{L}$ )	Found (Particles/ $\mu\text{L}$ )	Recovery (%)	RSD (%)
<b>20% Diluted ED-FBS</b>	$4.0 \times 10^4$	$3.85 \times 10^4$	96.25	3.21
	$4.5 \times 10^5$	$4.21 \times 10^5$	93.56	4.41
	$2.5 \times 10^6$	$2.52 \times 10^6$	100.8	2.89
<b>20% Diluted UC-Serum</b>	$4.0 \times 10^4$	$3.94 \times 10^4$	98.50	3.28
	$4.5 \times 10^5$	$4.69 \times 10^5$	104.2	5.25
	$2.5 \times 10^6$	$2.67 \times 10^6$	106.8	2.84
<b>20% Diluted UC-Urine</b>	$4.0 \times 10^4$	$3.69 \times 10^4$	92.25	5.40
	$4.5 \times 10^5$	$4.38 \times 10^5$	97.33	3.13
	$2.5 \times 10^6$	$2.58 \times 10^6$	103.2	3.30



**Table S4.** Clinical information of healthy donors and cancer patients.

<b>Clinical Condition</b>	<b>Number</b>	<b>Gender</b>	<b>Age</b>
<b>Healthy donors</b>	H1	Male	33
	H2	Male	23
	H3	Female	33
	H4	Female	30
	H5	Male	59
	H6	Female	59
	H7	Male	34
<b>Liver cancer</b>	P1	Male	68
	P2	Female	69
	P3	Male	65
<b>Cholangiocarcinoma</b>	P4	Female	52
	P5	Male	70
	P6	Male	77
<b>Breast cancer</b>	P7	Female	49
	P8	Female	55

## References

- (1) Li, B.; Ellington, A. D.; Chen, X. Rational, modular adaptation of enzyme-free DNA circuits to multiple detection methods. *Nucleic Acids Res.* **2011**, *39*, e110-e110.
- (2) Xia, Y.; Liu, M.; Wang, L.; Yan, A.; He, W.; Chen, M.; Lan, J.; Xu, J.; Guan, L.; Chen, J. A visible and colorimetric aptasensor based on DNA-capped single-walled carbon nanotubes for detection of exosomes. *Biosens. Bioelectron.* **2017**, *92*, 8-15.
- (3) Chen, Z.; Cheng, S.-B.; Cao, P.; Qiu, Q.-F.; Chen, Y.; Xie, M.; Xu, Y.; Huang, W.-H. Detection of exosomes by ZnO nanowires coated three-dimensional scaffold chip device. *Biosens. Bioelectron.* **2018**, *122*, 211-216.
- (4) Chen, X.; Lan, J.; Liu, Y.; Li, L.; Yan, L.; Xia, Y.; Wu, F.; Li, C.; Li, S.; Chen, J. A paper-supported aptasensor based on upconversion luminescence resonance energy transfer for the accessible determination of exosomes. *Biosens. Bioelectron.* **2018**, *102*, 582-588.
- (5) Fan, Y.; Duan, X.; Zhao, M.; Wei, X.; Wu, J.; Chen, W.; Liu, P.; Cheng, W.; Cheng, Q.; Ding, S. High-sensitive and multiplex biosensing assay of NSCLC-derived exosomes via different recognition sites based on SPRi array. *Biosens. Bioelectron.* **2020**, *154*, 112066.
- (6) Cheng, N.; Song, Y.; Shi, Q.; Du, D.; Liu, D.; Luo, Y.; Xu, W.; Lin, Y. Au@Pd nanopopcorn and aptamer nanoflower assisted lateral flow strip for thermal detection of exosomes. *Anal. Chem.* **2019**, *91*, 13986-13993.
- (7) Li, B.; Pan, W.; Liu, C.; Guo, J.; Shen, J.; Feng, J.; Luo, T.; Situ, B.; Zhang, Y.; An, T.; Xu, C.; Zheng, W.; Zheng, L. Homogenous magneto-fluorescent nanosensor for tumor-derived exosome isolation and analysis. *ACS Sensors* **2020**, *5*, 2052-2060.
- (8) He, F.; Wang, J.; Yin, B. C.; Ye, B. C. Quantification of exosome based on a copper-mediated signal amplification strategy. *Anal. Chem.* **2018**, *90*, 8072-8079.
- (9) Yu, X.; He, L.; Pentok, M.; Yang, H.; Yang, Y.; Li, Z.; He, N.; Deng, Y.; Li, S.; Liu, T.; Chen, X.; Luo, H. An aptamer-based new method for competitive fluorescence detection of exosomes. *Nanoscale* **2019**, *11*, 15589-15595.
- (10) An, Y.; Jin, T.; Zhu, Y.; Zhang, F.; He, P. An ultrasensitive electrochemical aptasensor for the determination of tumor exosomes based on click chemistry. *Biosens. Bioelectron.* **2019**, *142*, 111503.
- (11) Dong, H.; Chen, H.; Jiang, J.; Zhang, H.; Cai, C.; Shen, Q. Highly sensitive electrochemical detection of tumor exosomes based on aptamer recognition-induced multi-DNA release and cyclic enzymatic amplification. *Anal. Chem.* **2018**, *90*, 4507-4513.